Proc. Natl. Acad. Sci. USA
Vol. 84, pp. 1769–1773, April 1987
Biochemistry

Structure of human lactoferrin at 3.2-Å resolution

(metalloprotein structure/x-ray crystallography/transferrin iron coordination/binding proteins)

BRYAN F. ANDERSON*, HEATHER M. BAKER*, ELEANOR J. DODSON†, GILLIAN E. NORRIS*, SYLVIA V. RUMBALL*, JOYCE M. WATERS*, AND EDWARD N. BAKER*‡

*Department of Chemistry and Biochemistry, Massey University, Palmerston North, New Zealand; and †Chemistry Department, University of York, Heslington, York YO1 5DD, Great Britain

Communicated by Brian W. Matthews, November 10, 1986

ABSTRACT **The three-dimensional structure of human milk lactoferrin, a member of the transferrin family, has been determined crystallographically at 3.2-Å resolution. The molecule has two-fold internal homology. The N- and C-terminal halves form two separate globular lobes, connected by a short α-helix, and carry one iron-binding site each. Each lobe has the same folding, based on two domains of similar supersecondary structure, with the iron site at the domain interface. Each iron atom is coordinated by four protein ligands: two tyrosines, one histidine, and one aspartate. A probable CO_3^{2-} (or HCO_3^-) ion is suggested by the electron density, bound to iron and adjacent to an arginine side chain and a helix N terminus. The protein folding and location of the binding sites show marked similarities with those of other binding proteins, notably the sulfate-binding protein from *Salmonella typhimurium*.**

Lactoferrin [also known as lactotransferrin (1)] is a member of the family of iron-binding proteins that also includes transferrin and ovotransferrin (2, 3). These proteins are widely distributed in the physiological fluids of vertebrates. Although they have been the subject of intensive investigation over many years no definitive three-dimensional structural information has hitherto been available. All are monomeric glycoproteins with ≈700 amino acid residues and molecular weight ≈80,000. Each binds reversibly two iron atoms (as Fe^{3+}), concomitantly with two CO_3^{2-} (or HCO_3^-) ions. Notable features of their binding properties are (*i*) the synergistic relationship between cation and anion binding (4), (*ii*) the extremely tight binding of iron (binding constant ≈ 10^{20} for lactoferrin), and (*iii*) the fact that this tightly bound iron is nevertheless available *in vivo*, apparently through binding at specific receptors (5, 6).

The known or proposed biological functions of the transferrins depend on their iron-binding properties. Thus serum transferrin, the iron transport protein in plasma, provides an iron source for hemoglobin synthesis and other metabolic requirements. Lactoferrin, widely distributed through many exocrine secretions, notably milk, and an important component of leukocytes, has strong bacteriostatic properties (7). These result from its avidity for iron, depriving bacteria of iron essential for growth. It may also protect cells from free radical damage by binding potentially catalytic free iron (8).

All three proteins have bilobal structures. This is indicated by (*i*) fragmentation studies (ref. 9 and references therein), which demonstrate that the polypeptide chain can be cleaved into two halves, each carrying one iron site, and (*ii*) low-resolution x-ray studies (10). Amino acid sequence alignments (11) show that, in addition to the extensive homology between different transferrins, each also shows strong two-fold internal homology, indicative of gene duplication from a one-iron 40,000 molecular weight precursor molecule. For lactoferrin, there is ≈40% sequence identity between its N- and C-terminal halves.

Here we report the results of an x-ray analysis of the structure of human lactoferrin at 3.2-Å resolution, allowing a description of the polypeptide chain folding, and the nature and location of the iron sites. We also note a remarkable similarity between the organization of the lactoferrin molecule and that of certain other binding proteins.

Structure Determination

Lactoferrin was isolated from human milk and crystallized as the iron-saturated protein (Fe_2Lf) as described previously (12). To improve stability, these crystals, grown at low ionic strength (0.01 M sodium phosphate buffer, pH 7.8), in the presence of 10% (vol/vol) ethanol, were transferred to solutions containing 20% (vol/vol) 2-methyl-2,4-pentanediol. All the present work has been based on these methylpentanediol-equilibrated crystals. The crystals are orthorhombic, $a = 156.2$ Å, $b = 97.3$ Å, $c = 55.85$ Å, space group $P2_12_12_1$, with one molecule in the asymmetric unit. Three heavy atom derivatives, obtained by soaking crystals in solutions containing (*i*) 2 mM K_2PtCl_6 for 3 days, (*ii*) a saturated solution of $PtenCl_2$ (en = ethylenediamine) for 10 days, and (*iii*) 2 mM phenylmercuric acetate (PhHgOAc) for 3 days were used in the structure analysis.

Data for the native protein and its derivatives were collected at room temperature with an Enraf–Nonius CAD4 diffractometer equipped with a helium-filled diffracted beam path. Intensities were obtained from a limited step scan (in ω) through each reflection peak, with Gaussian profiles being fitted (13). Backgrounds, measured between reciprocal lattice points, for short times, were averaged in blocks of reciprocal space (14). In this way 2000–3000 reflections per day could be obtained, with merging R values of 3–5% for redundant measurements. Native crystal data to 3.2 Å (14,900 reflections) were measured from a single crystal (intensity fall-off ≈ 27% over 8 days). Derivative crystals were more radiation sensitive, three crystals being required for the K_2PtCl_6 derivative, two for $PtenCl_2$, and two for PhHgOAc. With crystals of size 1.2 × 0.8 × 0.8 mm, more than 85% of reflections in the outer 3.5- to 3.2-Å shell had $I > 2\sigma_I$.

Heavy atom sites were determined from difference Patterson and difference Fourier syntheses, and they were refined independently, using centric data only (coefficients $|\Delta F|_{iso}$) in a standard structure factor least-squares program. Some details are in Table 1. The two platinum derivatives share one major site of substitution but differ in their minor sites. The mercury derivative also uses this same major site but has five other almost equally occupied sites which differ from those of the platinum derivatives.

The publication costs of this article were defrayed in part by page charge payment. This article must therefore be hereby marked "*advertisement*" in accordance with 18 U.S.C. §1734 solely to indicate this fact.

Abbreviation: en, ethylenediamine.

‡To whom reprint requests should be addressed.

Table 1. Statistics for heavy-atom derivatives

Derivative	Resolution, Å	Merging *R* value	R_F	No. of heavy atom sites	Centric *R* value, R_c
K_2PtCl_6	3.2	0.044	0.136	9	0.49
$PtenCl_2$	3.5	0.040	0.127	6	0.50
PhHgOAc	3.5	0.041	0.187	6	0.62

Merging $R = \Sigma|I_h - \bar{I}_h|/\Sigma\bar{I}_h$, where $\bar{I}_h$ = mean value of I_{hkl}. R_F = fractional isomorphous difference = $\Sigma|\Delta F|_{iso}/\Sigma|F_P|$, where $|\Delta F|_{iso} = ||F_{PH}| - |F_P||$ and F_P and F_{PH} are observed native and derivative structure amplitudes. $R_c = \Sigma||F_{PH} - F_P| - |F_H||/\Sigma|F_{PH} - F_P|$ calculated for centric data only. F_H is the heavy-atom structure factor.

Phases were initially calculated to 3.5-Å resolution by using all three derivatives, with both isomorphous and anomalous differences included in the phase calculation. The mean figure of merit was 0.68. Subsequent electron density maps at 3.5 Å and 3.2 Å (with 3.5- to 3.2-Å phasing from the K_2PtCl_6 derivative only) contained encouraging features: two distinct globular lobes, quite long stretches of continuous chain, and one iron site clearly evident. The polypeptide chain could not be traced unambiguously, however, and it was clear that although phasing was good to ≈4.0 Å it deteriorated markedly towards 3.2 Å. Solvent flattening techniques, based on those of Wang (15), were then applied, using a conservative estimate of the solvent content (40%, compared with the actual value of ≈55%). The molecular envelope was defined by the reciprocal space algorithm of Leslie (16). This involves the use of structure factors, derived from the initial electron density map and modified by the chosen averaging sphere, to calculate the envelope mask. An 8-Å averaging sphere was used (a 10-Å sphere was found to cut through obvious protein density). Initial phases were the 3.2-Å multiple isomorphous replacement phases. After four cycles of solvent flattening, map inversion, and phase combination, convergence was reached. The envelope mask was recalculated and four more cycles led again to convergence.

The mean figure of merit to 3.2 Å was 0.75 after these procedures, and although the mean phase shift was not great (18.7° for noncentric reflections) the resultant map was a significant improvement on the original multiple isomorphous replacement map. Its quality can be judged from Fig. 1; most noticeable was the improved side-chain density, but all of the protein density was sharpened, and in critical places connections were clarified. Both iron atoms stood out clearly, and a three-turn helix linking the two lobes was apparent. This was used as the starting point for tracing the chain in both directions. The amino acid sequence (11) was invaluable; aromatic side chains had bulky well-resolved density, and other types of side chains were seen to conform with expected protein structural roles and environments. The 16 disulfide bridges were also of great assistance as markers. In the final tracing there are two significant breaks in the chain, both in the C-terminal lobe (residues 388–403 and 429–433 have no density). The N-terminal residues 1–5 are also not visible. In several other places the density is broken or indistinct over one or two residues, but the connectivity remains unambiguous. The two lobes were traced independently. Both were found, however, to have essentially the same folding (see below), consistent with their sequence homology, and sections that were poorly defined in one lobe were often well defined in the other. Major sites of heavy atom substitution are all adjacent to potential protein ligands (e.g., the major platinum-binding site lies between the side chains of His-602 and Met-605, while the next three highest-occupancy platinum sites are adjacent to Met-615, His-92, and His-627). Similarities and differences in the transferrin and ovotransferrin sequences are also consistent with our present interpretation (see below). The N lobe has been fitted to the density in a Richards box, and a detailed model of the entire molecule has been fitted on an Evans and Sutherland PS 300 interactive graphics system.

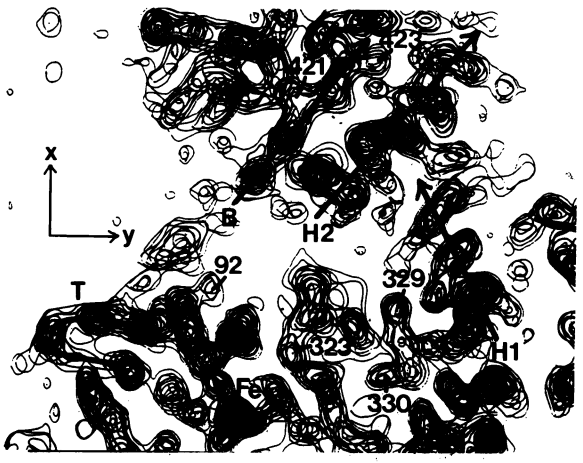

FIG. 1. A 7-Å-thick slice of electron density in the region of the boundary between the N lobe (bottom) and the C lobe (top). Information is taken from the 3.2-Å lactoferrin map after solvent flattening; sections are down the *z* axis. Note the connecting helix 333–343 (H1). Other features indicated include an N-lobe β-turn 85–88 (T), a C-lobe helix 618–633 (H2) and β-strand 420–428 (B), and side chains of His-92, Tyr-323, Asn-329, Leu-330, Pro-421, and Leu-423. The N-lobe iron atom is at bottom.

Organization of the Lactoferrin Molecule

The molecule is folded into two globular lobes, the N lobe, comprising the N-terminal half of the polypeptide chain (residues 1–332), and the C lobe (the C-terminal half, residues 344–703). They are connected by a three-turn helix, residues 333–343. Each lobe is an ellipsoid of approximate dimensions 55 × 35 × 35 Å; the two lobes are then joined with their long axes roughly antiparallel (angle of ≈150° between them), as in Fig. 2. One lobe may be superimposed on the other by a rotation of ≈180°, coupled with a translation.

Each lobe is further subdivided into two equal-sized domains, so that the molecule as a whole consists of four domains, N_I, N_{II}, C_I, and C_{II} (Fig. 2). The basic folding pattern found in *both* lobes is illustrated in Fig. 3. The first 90–100 residues (N-lobe 1–90; C-lobe 343–444) are part of domain I. The next 160–170 residues (N-lobe 91–251; C-lobe 445–608) form domain II. The chain then crosses back to domain I, where the next 70 or so residues (N-lobe 252–320; C-lobe 609–676) complete its folding. Finally, a helix (N-lobe

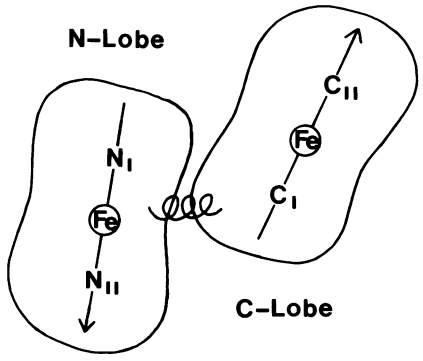

FIG. 2. Relative dispositions of the N-terminal and C-terminal lobes in lactoferrin. The two domains in each lobe are labeled.

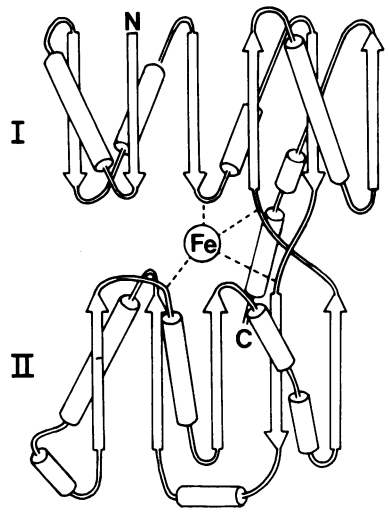

FIG. 3. Schematic representation of the folding pattern in each lobe of lactoferrin. Domain I is based on a β-sheet of four parallel and two antiparallel strands; domain II, four parallel and one antiparallel strands.

320–331; C-lobe 676–690) runs back across the domain interface to domain II.

The domains have similar supersecondary structures: irregular twisted β-sheets of similar topology, covered on either side by connecting loops and helices (Fig. 3). Crossover connections between parallel β-strands are all right-handed, as expected (17), and include helices running antiparallel to the β-strands. This places the C termini of the parallel β-strands and the N termini of the α-helices close to the interface between the two domains. Two strands of chain (residues 78–100 and 244–257 in the N lobe; 418–454 and 601–614 in the C lobe) run the full length of the lobe, contributing to both β-sheets. These two "backbone" strands may provide a flexible hinge between the domains. The overall levels of secondary structure in the molecule are ≈32% helix and ≈22% β-sheet.

A C_α-plot of the N lobe is shown in Fig. 4. The N and C lobes superimpose with an rms deviation of 2.2 Å (for 90% of C_α positions); agreement should be closer still when the structure is refined. Minor differences in the two lobes accompany insertions or deletions in one lobe relative to the other; these occur in external loops and do not disturb the basic folding. Of the 16 disulfide bridges, 6 pairs are equivalent in the two lobes (Fig. 5). The other 4 are all in the C lobe. One (439–661) is associated with a 10-residue insertion, and another (639–644) joins residues already close together in the N lobe. The remaining two (417–698 and 495–689) cause the C-terminal residues, 689–703, to fold over the surface of the C lobe and in doing so appear to reduce access to the C-lobe iron site. The equivalent section of chain at the C terminus of the N lobe projects from it as the connecting helix, 333–343.

The sites of carbohydrate attachment, one in each lobe (at Asn-137 and Asn-490), are on the surface of the molecule, at the C termini of two homologous helices (residues 121–137 and 477–492). Both are adjacent to quite large solvent regions in the crystal, and although some weak density extends beyond the asparagine side-chain density, the carbohydrate is either disordered or has had its density drastically reduced by the solvent flattening procedures. Refinement of the structure should clarify this point.

Iron-Binding Sites

The iron sites, one in each lobe, are about 42 Å apart (Fig. 5). Both occupy equivalent locations, at the interface between the two domains of the lobe (Fig. 4). Although the iron is itself buried, its immediate environment within the domain interface is quite hydrophilic.

Each iron atom is coordinated to four protein ligands, the phenolate oxygens of Tyr-93 and Tyr-191 (Tyr-447 and Tyr-540 in the C lobe), the $N_{\varepsilon 2}$ imidazole nitrogen of His-252 (His-609) and a carboxylate oxygen of Asp-61 (Asp-407) (Fig. 6). Many spectroscopic and model studies have previously implicated tyrosine and histidine ligands (refs. 2 and 18 and references therein). Although the coordination of a carboxylate group was not predicted from such studies, it is consistent with the strong preference for binding high-spin Fe(III). All four ligating residues are conserved in lactoferrin, serum transferrin, and ovotransferrin, in both halves of each molecule, indicating that they are likely to be iron ligands in all transferrins. Two other invariant residues, Tyr-83 (427) and His-117 (472), suggested as potential ligands by sequence homology (11), are close to the iron site but are not ligands.

The four protein ligands occupy four of the six octahedral sites around each iron. Two *cis* positions remain, leaving an "open" side of the iron atom for coordination by the anion, or a water molecule, or both. In each iron site additional density is found to protrude from the iron density, spanning these two positions. Magnetic resonance studies (19) favor direct coordination of the anion, and this extra density can be fitted very satisfactorily by a CO_3^{2-} (or HCO_3^-) ion coordi-

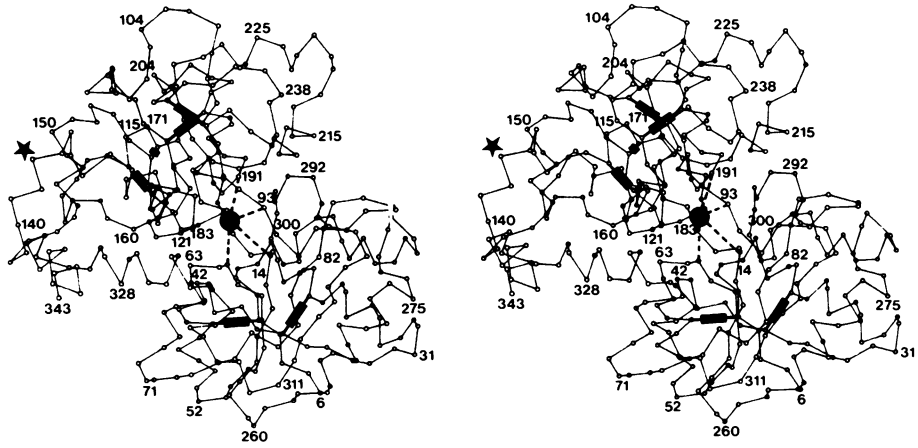

FIG. 4. Stereo C_α diagram of the N lobe of lactoferrin, showing the iron atom (●) between the two domains. Domain I (residues 6–90 + 252–320) is at the bottom, domain II (residues 91–251) is at the top. Disulfide bridges (▬) are shown and the carbohydrate attachment site (★) is indicated.

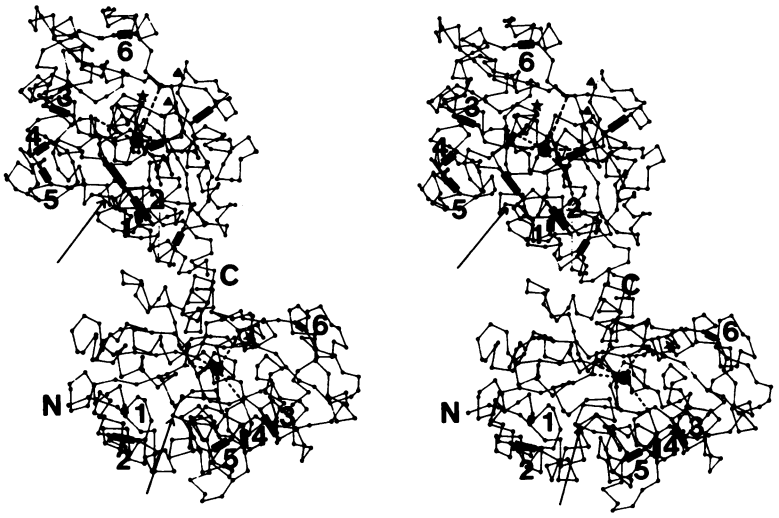

FIG. 5. Stereo C_α plot of the whole lactoferrin molecule. N and C termini (residues 6 and 703) are labeled. The iron atoms, 42 Å apart, are shown as ●; disulfide bridges, as ▬. The six homologous disulfides (common to lactoferrin, transferrin, and ovotransferrin, in both lobes) are numbered as in ref. 11. Carbohydrate attachment sites are indicated (★, lactoferrin and ▲, transferrin). Approximate locations of "equivalent" channels leading to the anion site in each lobe are arrowed; note their inequivalence in terms of the molecule as a whole.

nated in bidentate fashion to the iron. It is adjacent to (*i*) the side chain of Arg-121 (477), which is presumably the arginine identified in chemical modification studies (20) as essential for iron binding, and (*ii*) the N terminus of the α-helix 121–137 (477–492). Full details of the anion-binding interactions and proper assignment of the density round the iron (whether due to the anion, or anion plus water molecule) must await refinement at higher resolution. At present, however, our putative anion position bridges between iron and protein, as has often been suggested (e.g., ref. 4).

Implications for Iron Binding and Release

There is evidence for all transferrins that a significant conformational change accompanies iron binding, with the structure becoming markedly more compact (21). This may be necessary to prevent hydrolysis of the bound Fe(III). The location of each iron site, between two domains, suggests that the conformational change could involve hinging of the domains, which close over the iron atom as it binds. The construction of each site lends support to this idea. The ligands come from three different parts of the structure, one (Asp-61) from the body of domain I, a second (Tyr-191) from the body of domain II, and the remaining two (Tyr-93 and His-252) from the two "backbone" strands of chain as they run past the iron. A possible sequence is that the iron binds to domain II and the "backbone" ligands while the protein is in an "open" configuration [the fragment 91–257, which corresponds essentially to domain II, is known to bind iron (9)] and then binds to the remaining ligand, Asp-61, as domain I closes over it. The anion, which is believed to bind first (2, 19), would be involved through its bridging between the metal ion and domain II, thus explaining the synergistic relationship between anion and metal binding.

Release of iron may involve the access of small molecules or ions to the iron site. A consequence of the relationship between N and C lobes is that regions which are structurally equivalent are not equivalent in terms of the molecule as a whole. Thus approach to Arg-477 and the anion site in the C lobe appears more restricted than to the equivalent site in the N lobe, because the access "channel" is close to the interface between the lobes (see Fig. 5). This, together with the structural difference at the C terminus (see above) and variations in some residues around the iron sites, could account for the greater stability of the C-lobe site towards protonation, compared with the more acid-labile N-lobe site (2). The lack of symmetry in the molecule as a whole could also result in differences in the accessibility of recognition sites on the two halves of the molecule, as well as differences in the binding properties of the two iron sites.

Comparison with Other Proteins

The lactoferrin structure is consistent with known structural data on transferrin and ovotransferrin. Sites of insertions or deletions in one protein or other correspond to surface loops in lactoferrin, and the secondary structure elements show strong sequence conservation. The carbohydrate sites in

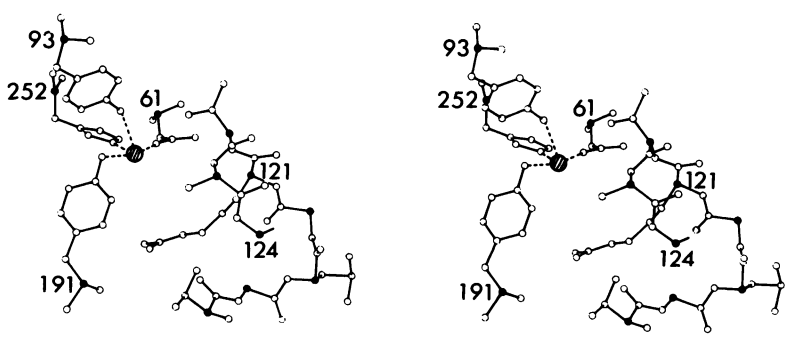

FIG. 6. Stereo view of the iron coordination in lactoferrin. Only the protein ligands are shown. Density that may be attributable to the CO_3^{2-} anion, and possibly a water molecule as well, spans the two remaining octahedral coordination positions (left vacant here).

serum transferrin [which differ from lactoferrin and ovotransferrin (11)], correspond to surface loops in lactoferrin (Fig. 5). Both are in the C lobe, spatially close together (≈13 Å apart), but ≈30 Å from the nearest carbohydrate site in lactoferrin. The four extra disulfide bridges in serum transferrin all link sections of chain that are already adjacent in the lactoferrin structure. Two (134–335 and 341–620, lactoferrin numbering) are at either end of the connecting helix between lobes. Although the three-dimensional structures of transferrin and ovotransferrin seem certain to be very similar to the structure of lactoferrin, there are relatively few interactions across the interface between the N and C lobes (those that do exist involve mainly the two helices 320–331 and 693–703). Thus the relative orientations of the two lobes could vary. Likewise if hinging of the two domains within a lobe accompanies metal binding, the extent of closure over the iron could vary, in response to sequence changes in the domain interface.

Finally, there is an unexpected similarity between the structure of lactoferrin and the structures of other binding proteins, the bacterial periplasmic binding proteins specific for L-arabinose (22), D-galactose (23), leucine/isoleucine/valine (24), and sulfate (25). Each of these proteins is similar in size to a single lobe of lactoferrin (≈300 residues). All have ellipsoidal two-domain structures in which the substrate binds between the domains. The two domains have similar folding: β-sheets of five or six strands, covered on either side by connecting helices such that the C termini of the parallel strands and the N termini of the helices point towards the binding site cleft between domains; and three peptide segments linking the domains, two contributing to the β-sheets, the third being the C-terminal segment. The most striking resemblance is between lactoferrin and the sulfate-binding protein (SBP) of *Salmonella typhimurium*. Both have precisely the same sheet topology, many helices match, and there are similarities in anion binding—in lactoferrin the N terminus of helix 121–137 points at the putative CO_3^{2-} ion, and in SBP the equivalent helix 131–146 is a major contributor to binding SO_4^{2-} (although in SBP other helices, from *both* domains, also contribute to anion binding, and the anion site appears further from the "backbone" strands).

The above binding proteins, like lactoferrin, must bind a substrate with high affinity but also release it at specific receptors. In each case a conformational change involving hinge bending between the domains is believed to be involved. Whether the structural similarities represent evolutionary divergence from an ancestral binding protein (prior to the gene doubling that produced the bilobal transferrins) or whether they simply reflect a highly suitable folding pattern for binding proteins will require more detailed analysis to assess.

We gratefully acknowledge many people who have helped and supported this work, especially Prof. Brian W. Matthews for use of data collection facilities in his laboratory (by E.N.B.) during an enjoyable period of study leave at the University of Oregon, Prof. G. G. Dodson of the University of York for the use of his laboratory computing and interactive graphics facilities, colleagues at Massey University for their support and encouragement, and the mothers and hospital staff who provided milk. We are also very grateful for financial support from the Medical Research Council of New Zealand, the New Zealand Dairy Research Institute, the University Grants Committee, and Massey University.

1. Montreuil, J., Tonnelat, J. & Mullet, S. (1960) *Biochim. Biophys. Acta* **45**, 413–421.
2. Aisen, P. & Listowsky, I. (1980) *Annu. Rev. Biochem.* **49**, 357–393.
3. Brock, J. H. (1985) *Top. Mol. Struct. Biol.* **7**, 183–262.
4. Schlabach, M. R. & Bates, G. W. (1975) *J. Biol. Chem.* **250**, 2182–2188.
5. Cox, T. M., Mazurier, J., Spik, G., Montreuil, J. & Peters, T. J. (1979) *Biochim. Biophys. Acta* **588**, 120–128.
6. Davidson, L. A. & Lonnerdal, B. (1985) *Fed. Proc. Fed. Am. Soc. Exp. Biol.* **44**, 1673 (abstr.).
7. Bullen, J. J., Rogers, H. J. & Leigh, L. (1972) *Br. Med. J.* **3**, 69–75.
8. Baldwin, D. A., Jenny, E. R. & Aisen, P. (1984) *J. Biol. Chem.* **259**, 13391–13394.
9. Legrand, D., Mazurier, J., Metz-Boutigue, M.-H., Jolles, J., Jolles, P., Montreuil, J. & Spik, G. (1984) *Biochim. Biophys. Acta* **787**, 90–96.
10. Gorinsky, B., Horsburgh, C., Lindley, P. F., Moss, D. S., Parkar, M. & Watson, J. L. (1979) *Nature (London)* **281**, 157–158.
11. Metz-Boutigue, M.-H., Jolles, J., Mazurier, J., Schoentgen, F., Legrand, D., Spik, G. & Jolles, P. (1984) *Eur. J. Biochem.* **145**, 659–676.
12. Baker, E. N. & Rumball, S. V. (1977) *J. Mol. Biol.* **111**, 207–210.
13. Hanson, J. C., Watenpaugh, K. D., Sieker, L. & Jensen, L. H. (1979) *Acta Crystallogr. Sect. A* **35**, 616–621.
14. Baker, E. N. (1977) *J. Mol. Biol.* **115**, 263–277.
15. Wang, B. C. (1985) *Methods Enzymol.* **115**, 90–112.
16. Leslie, A. G. W. (1987) *Acta Crystallogr. Sect. A* **43**, 134–136.
17. Richardson, J. S. (1976) *Proc. Natl. Acad. Sci. USA* **73**, 2619–2623.
18. Chasteen, N. D. (1983) *Trends Biochem. Sci.* **8**, 272–275.
19. Zweier, J. L., Wooten, J. B. & Cohen, J. S. (1981) *Biochemistry* **20**, 3505–3510.
20. Rogers, T. B., Borresen, T. & Feeney, R. E. (1978) *Biochemistry* **17**, 1105–1109.
21. Rossenau-Motreff, M. Y., Soetewey, F., Lamote, R. & Peeters, H. (1971) *Biopolymers* **10**, 1039–1048.
22. Gilliland, G. L. & Quiocho, F. A. (1981) *J. Mol. Biol.* **146**, 341–362.
23. Vyas, N. K., Vyas, M. N. & Quiocho, F. A. (1983) *Proc. Natl. Acad. Sci. USA* **80**, 1792–1796.
24. Saper, M. A. & Quiocho, F. A. (1983) *J. Biol. Chem.* **258**, 11057–11062.
25. Pflugrath, J. W. & Quiocho, F. A. (1985) *Nature (London)* **314**, 257–260.